ARTICLE

Investigation on Thermal Insulation and Mechanical Strength of Lightweight Aggregate Concrete and Porous Mortar in Cold Regions

Jianan Wu[1], Ke Xue[2], Zhaowei Ding[3], Lei Lang[3], Kang Gu[3], Xiaolin Li[4], Mingli Zhang[5] and Desheng Li[3,6,*]

[1]Ningbo City College of Vocational Technology, Ningbo, China

[2]College of Water Conservancy and Hydropower Engineering, Sichuan Agricultural University, Ya'an, China

[3]State Key Laboratory of Ocean Engineering, Shanghai Jiao Tong University, Shanghai, China

[4]College of Civil Engineering and Architecture, Jiaxing University, Jiaxing, China

[5]Department of Civil Engineering, Lanzhou University of Technology, Lanzhou, China

[6]Department of Civil Engineering, College of Science, Nanjing University of Science and Technology, Nanjing, China

[*]Corresponding Author: Desheng Li. Email: ridson319@sjtu.edu.cn

ABSTRACT

Thermal insulation is an important indicator to evaluate the construction material in cold region engineering. As we know, adding the industrial waste as lightweight aggregate or creating the pore inside the cement-based composite could make the texture loose, and the thermal insulating capacity of the material would be improved with this texture. Using these methods, the industrial by-product and engineering waste could be cycled in an efficient way. Moreover, after service the fragmented cement composites paste could be used as aggregate in the thermal insulating concrete again. While the porous texture is not favorable for the mechanical strength and long-term durability in a cold environment. To balance the above three requirements from two opposite directions, different processing methods were applied to create the thermal insulation concrete/mortar. Firstly, the organic/inorganic lightweight aggregate, including the Expanded Polystyrene (EPS), Expanded Perlite (EP), and Ceramsite (CRMST) particles, were applied to create the Lightweight Aggregate Concrete (LWAC). As the comparative tests, the expanded Superabsorbent Polymer (SAP) hydrogel and Air-Entraining Agent (AEA) were also introduced to create the porous mortar. The above concrete/mortar was tested in the normal state and under the Freeze-Thaw cycle to explore the engineering performance in cold regions. During the experimenting process, the thermal insulation, mechanical strength, and frost resistance of these cement-based composites were investigated, and an optimal thermal insulation concrete/mortar was determined.

KEYWORDS

Thermal insulation; mechanical strength; cement-based composite; freeze-thaw cycle; frost resistance

1 Introduction

Climate change is growing drastically around the world, and the threat from the climatic disaster deserves more attention [1–4]. The freezing rain [5] in Southwestern China and the cold surge activity [6] in Southeastern China are very dangerous to human life and properties, which are the manifestation of the

climate change or La Nina [7]. Faced with the above disasters, local people should be well-prepared. While the rural residential buildings in Southern China seldom take thermal insulation into consideration [8]. Moreover, the rural residential buildings make the winter heating in a low efficient way. They usually resort to an air conditioner when the air temperature drops to 0°C. While the poor sealing ability and thermal insulating ability of the rural building in North China would not be advantageous to the above heating way. For example, the tiled roof and single layer glass are not good for heat preservation [9]. Hence in response to climate change, the cement-based material with a good thermal insulation and mechanical strength would largely increase the energy efficiency and extend the service life of the engineering structures, which is of great importance to carbon neutral goal and the environment-friendly society [10–12].

Good thermal insulation is generally accompanied with poor mechanical performance for the cement-based materials [13]. From the view of microstructure, the good thermal insulation of material basically relates to the incompactness of the paste [13,14]. Hence, achieving an optimum combination for both thermal insulation and mechanical properties becomes the most important and difficult issue for the materials used in cold regions engineering [15].

Some researchers believe that the cement-based composite with a good thermal insulation must compromise to have a poor mechanical performance [13,16,17]. After comparing and analyzing the physical and mechanical properties of some cement-based composite and their microstructure, it is found that the concrete/mortar with a porous and loose microstructure could achieve that goal. Many methods were tried to enhance the thermal insulation of the cement-based material at the expanse of the minimum mechanical strength loss, for example replacing the cement with the mineral admixture [18], adding the porous lightweight aggregate [13], and increasing the porosity of mortar paste [14,19].

Demirboğ found that the thermal conductivity decreased with the replacement of cementitious material. The maximum thermal conductivity reduction (30%) occurred at the 30% fly ash replacement, while the highest compressive strength occurred at 15% blast furnace slag replacement [18]. The addition of lightweight aggregate is more common in engineering structures. Pia et al. [14] made use of clay and wood aggregate to enhance the thermal insulation. Ünal [13] added diatomite to increase the thermal insulation of the lightweight aggregate concretes and found that the concrete with 30% fine, 40% medium, and 30% coarse aggregate could improve both the thermal insulation and compressive strength. Marie [20] used crumb rubber as fine aggregate and found that 30% replacement of coarse aggregate with the recycled concrete aggregate, together with 10% replacement of fine aggregate with the crumb rubber could make the thermal conductivity lower than the traditional concrete.

For the economic and recycled merits, the lightweight aggregate concrete is utilized in this study. The lightweight aggregates are generally the industrial by-product or engineering waste, which are reused in order to avoid the environmental pollution or waste dumping [21,22]. The lightweight aggregates could be reused as the lightweight aggregate in the thermal insulation concrete [23,24]. Moreover, the fragmented paste of the lightweight aggregate concrete and porous mortar after service life could be reused as the thermal insulating aggregate [25]. It is of importance to the sustainable development in building industrial and environmental protection. The lightweight aggregate concrete also has an advantage that comparatively lighter dead weight of building structure could reduce the risk of earthquake acceleration [26]. Whereas, the loose and porous texture of the lightweight aggregate concrete compromises to have a poor mechanical performance in engineering applications. The Freeze-Thaw cycle in the cold regions also reduces the long-term service of the lightweight aggregate concrete to a large extent. Hence, the thermal insulation, mechanical strength, and the frost resistance in a cold environment were tested in this study. Several kinds of common lightweight aggregates were introduced to pursue an optimal performance.

As the comparative tests, the porous mortars were also used in this study. The air-entraining agent was added to induce the micro-voids inside the mortar paste, which could improve the thermal insulation. Besides that, the Superabsorbent Polymer (SAP) was also utilized to create the porous mortar. SAP particle was pre-expanded before the mixing process, then the cavities were created by the expanded SAP hydrogel after the mortar hardening. Moreover, the expanded SAP hydrogel sustainably released water during the hardening process. The secondary water participation accelerates the further hydration of unhydrated cement inside the mortar paste. Hence, the content of the crystalline product would be increased [27]. As the previous research indicates, the mortar with a crystalline microstructure would increase the mechanical strength and frost durability under the Freeze-Thaw cycle. Even the internal curing mortar has a higher thermal conductivity than amorphous and vitreous material [28,29], the thermal insulation is still satisfactory.

During the entire experimenting process, the dry density, net water absorption, flexural strength, and compressive strength were measured. Besides, the microstructure was observed through the optical microscope and scanning electron microscope to analyze the thermal and mechanical characteristics. Before and after the Freeze-Thaw cycle, the mechanical strength of these composites was compared to investigate the frost resistance. The frost-resisting mechanism of the concrete/mortar was also explored.

2 Materials and Methods

2.1 Raw Materials

The Portland cement 42.5 R compliant with the requirement of EN 197-1 was used, and the density is 2.95 g/cm^3. The chemical composition of the cement used in this study is listed in Table 1. The fine aggregate was the standard sand. The designed water/cement/sand ratio is 1:2:6 for each testing group. Whether to add or reduce the water dosage depended on the water absorption of the coarse aggregate. Detailed information of the concrete/mortar paste was shown in Table 2.

Table 1: The chemical compositions (by % weight) of raw materials

Material	CaO	SiO$_2$	Al$_2$O$_3$	Fe$_2$O$_3$	Na$_2$O	MgO	K$_2$O	Others
OPC	64.44	21.60	4.13	4.57	0.11	1.06	0.56	0.76

Table 2: Detailed experimental design

No.	Water	Cement	Sand	aggregate/additives	Aggregate diameter	Aggregate volume	Label
Unit	g	g	g	-		ml	-
1	160	300	900	coarse expanded perlite	2 mm	360	CEP-1
2	200	300	900	coarse expanded perlite	2 mm	360	CEP-2
3	200	300	900	medium expanded perlite	1 mm	360	MEP
4	160	300	900	air-entraining agent	-	-	AEA
5	160	300	900	expanded polystyrene	4 mm	360	EPS
6	160	300	900	expanded SAP hydrogel	-	360	SAP
7	160	300	900	ceramsite particle	5 mm	360	CRMST

2.2 The Lightweight Aggregate and Artificial Pore Inducing Agent

In this research, different kinds of lightweight aggregates, which have a good thermal insulating capacity, were introduced into the cement-based composite, including Expanded Polystyrene (EPS), Expanded Perlite (EP), and Ceramsite (CRMST). The aggregate diameter mean is generally smaller than

4.75 mm. Hence in this study, they were classified as medium aggregate instead of coarse aggregate. The aggregate content for each testing group was based on the volume fraction in the concrete specimen, which was designed as 360 ml (Table 2).

As the comparison specimen, the expanded SAP hydrogel and air-entraining agent (AEA) were also applied to create the porous mortar. The SAP particles were pre-expanded with water to a volume of 360 ml, and then added into the cement-sand dry mix. The AEA was added after the dry mixing process. Similar to the light aggregate concrete, the dosages of SAP and AEA were designed to induce the pore equal to a volume of 360 m. While the density and porosity of mortar prisms for each testing group could not be guaranteed the same, it depends on the measured data after the concrete/mortar hardening.

2.3 Specimen Preparation

The cement, sand, and aggregate were dry-mixed for 1 min to ensure the aggregate disperse uniformly. Then water was added, and the water dosage was adjusted depending on the requirement for basically satisfactory fresh properties. The concrete/mortar specimen was $40 \times 40 \times 160$ mm^3 prism. After 24 h's hardening process, the specimen was demouled and placed into a chamber where the air temperature was $25 \pm 2°C$ and the relative humidity was $80 \pm 5\%$ for 28 days' curing.

2.4 Experiment Design

Firstly, the basic physical properties of the concrete/mortar prism were measured, including the unit weight (UW), specific porosity (SP), and water absorption (WA), which were according to the Archimedes principle [30]. The above physical properties were measured on the 7th day, as shown in Fig. 1.
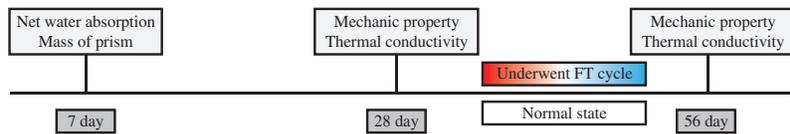
Figure 1: The entire experimenting process of this study

To know the mechanical strengthens and thermal insulating performance of the cement-based composite in clod region engineering, the thermal conductivity and mechanical properties were measured both on the 28th and 56th day. To investigate the frost resistance of the composites, the mechanical strength was measured in the normal state and after the Freeze-Thaw cycle on the 56th day (Fig. 1). FT is short for Freeze-Thaw. The Freeze-Thaw cycle was conducted on the 30th day. Hence, the influence from the Freeze-Thaw cycle could be understood through the mechanical strength comparison between the specimens in normal state and under the Freeze-Thaw cycle. To ensure the workability of the above thermal insulating concrete/mortar in cold regions, the investigation on the thermal performance, mechanical properties, and durability was conducted concurrently. Only in this way can the optimum thermal insulating concrete/mortar be obtained.

Though the main cause for porous texture is the type of lightweight aggregates and the voids volume inside the concrete/mortar paste, the water dosage during the mixing process still plays an important role. Hence, the water for expanded perlite groups were added in different dosages to explore the influence of w/b ratio or water dosage on the thermal insulation and the mechanical strength of the lightweight aggregate concrete. As shown in Fig. 2, the prism sections indicated the dissimilarity of the concrete paste, which were added with different dosage of water (CEP-1 and CEP-2).
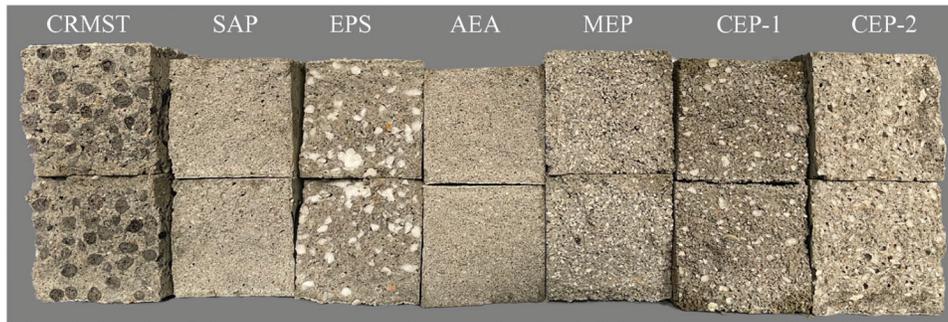
Figure 2: The sectional profile after flexural testing and the optical microscope

The Freeze-Thaw cycle in this study was featured with water involvement, which could also be named as the Thaw-Soak-Freeze cycle in other related researches [31]. The role of water in the degradation process of cement composite was not required to be researched. The water soaking process in the Freeze-Thaw cycle was just utilized to accelerate the degradation of the concrete/mortar prism. One Freeze-Thaw cycle included 4 h' freezing, 2 h' thawing, and 2 h' water soaking, which has been depicted in the previous publication [31]. The ambient temperature for the freezing stage and thawing stage was −20°C and 70°C, respectively. From the thawing stage to the freezing stage, there was a water soaking stage with the ambient temperature of 20°C, which was designed to guarantee the frost damage with sufficient water supply. Two Freeze-Thaw cycles were conducted for each day since the experiment started, and the Freeze-Thaw process was sustained for 10 days.

To figure out some interesting questions, the light aggregate or porosity-inducing agent was added following the below instruction. Detailed experimental design refers to Table 2:

(1) To explore the role of water dosage in the thermal insulating and mechanical performance of the lightweight aggregate concrete, the water of different dosages was added during the mixing process (160 ml for CEP-1 and 200 ml for CEP-2). The lightweight aggregate is the coarse expanded perlite with a mean diameter of 2 mm approximately.

(2) To explore the particle size of lightweight aggregate, the perlites aggregate with different diameters were used, namely the 2 mm coarse expanded perlite in CEP-2 and the 1 mm medium expanded perlite in MEP. The water dosage was kept constant.

(3) To compare the thermal insulation of organic and inorganic lightweight aggregate, the expanded polystyrene was added to compare with the expanded perlite and ceramsite. The test contrast was between CEP-1, EPS, and CRMST, whose water dosages are all 160 ml.

(4) To investigate the thermal insulation of the lightweight aggregate and artificial pore in the cement composite, the thermal conductivity of the expanded perlite, expanded polystyrene, and ceramsite added concrete were compared with the air-entraining agent (AEA) mortar and superabsorbent polymer (SAP) mortar. The test contrast was between CEP-1, EPS, CRMST and AEA, SAP, which shared the same water dosage of 160 ml.

(5) To explore the thermal and mechanical property of the porous mortar induced by air-entraining agent and SAP internal curing, the AEA mortar and SAP mortar were contrasted and analyzed.

2.5 Thermal Conductivity

The thermal conductivity of each testing group was measured 6 times and then averaged. To ensure the reliability of the measured value, the thermal conductivity was measured in the different directions (Fig. 3). After the first three measurements, both specimens were rotated and measured three more times in the

perpendicular direction. The measuring apparatus was the portable thermal conductivity meter TC 3000E following the standard ASTM C1113, as shown in Fig. 3. The measuring accuracy is ± 3%, and the measurement resolution is 0.0005W/(m·K).
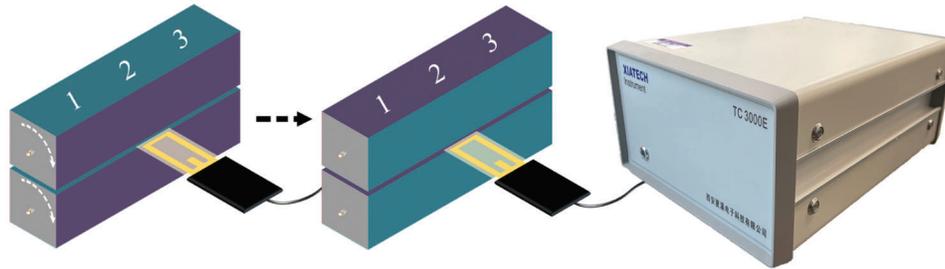
Figure 3: The schematic of the thermal conductivity measurement and the apparatus

2.6 Comparing Methods

In this study, the thermal insulation, mechanical strength, and frost resistance are of equal importance to the building material in cold regions. The flexural strength, compressive strength, thermal conductivity, and the flexural/compressive strength loss after the Freeze-thaw cycle were required to be compared among the cement composites used in this study. However, these parameters have different dimensions, which means they cannot be compared directly. In this paper, two methods were introduced to compare the above 5 parameters, including the separate standardized comparison and the integral comparison.

The standardized comparison

To quantify these above-mentioned 5 parameters, they were processed using the below equation. FS, CS, TC, FSS, and CSS are short for the flexural strength, compressive strength, thermal conductivity, and the flexural/compressive strength storage, which denote the subscript of the processed index for the standardized comparison. The flexural strength storage and compressive strength storage were namely the strengthen after the Freeze-Thaw cycle.

$$K_P = \frac{P - P_{\min}}{P_{\max} - P_{\min}} \times 100\% \qquad (1)$$

where K_P denotes the processed index for FS, CS, TC, FSS, and CSS, for example, the processed index for the flexural strength is K_{FS}. $P_{\max}$ and $P_{\min}$ denote the maximum and minimum of parameter P, for example, the maximum and minimum for the parameter FS are FS_{max} are FS_{min}. It should be noted that this equation is suited for the parameters whose higher value is beneficial for the material performance, such as the flexural strength, compressive strength, and the flexural/compressive strength storage. While for the thermal conductivity, whose lower value is beneficial for the thermal insulation, the equation should be revised as below:

$$K_P = \frac{P - P_{\max}}{P_{\min} - P_{\max}} \times 100\% \qquad (2)$$

The integral comparison

Except for the separate standardized comparison method, a holistic index was urged. As we know, both the thermal insulation and mechanical strength are of great importance for the cement-based composite in cold region engineering. The mechanical strength with a higher value and the thermal conductivity of a lower value are recommended. Hence, the above parameters are inputted into a formula to get a holistic index to combinatorically compare the integral performance of the lightweight aggregate concrete or

porous mortar in a cold environment. The equation to obtain the holistic index *KS* is given as below.

$$KS = \frac{Flexural\ strength \times Compressive\ strength}{Thermal\ conductivity} \tag{3}$$

2.7 Microstructure

To observe the microstructure and micromorphology of the selected testing samples, as well as to investigate the degradation mechanism of lightweight aggregate concrete and porous mortar, the microstructure analysis was conducted using the COXEM EM-30 Plus Scanning Electron Microscope (SEM). Before taking SEM photos, it should be noted that the testing mortar/concrete samples required to be coated with gold.

3 Results

3.1 Unit Weight and Specific Porosity

From Fig. 4, it is found that the SAP mortar specimen has the highest dry density, and the AEA mortar specimen comes the second. Then, the lightweight aggregate concretes follow. In other words, the dry density of the porous mortar specimen is comparatively higher than that of the lightweight aggregate concrete.
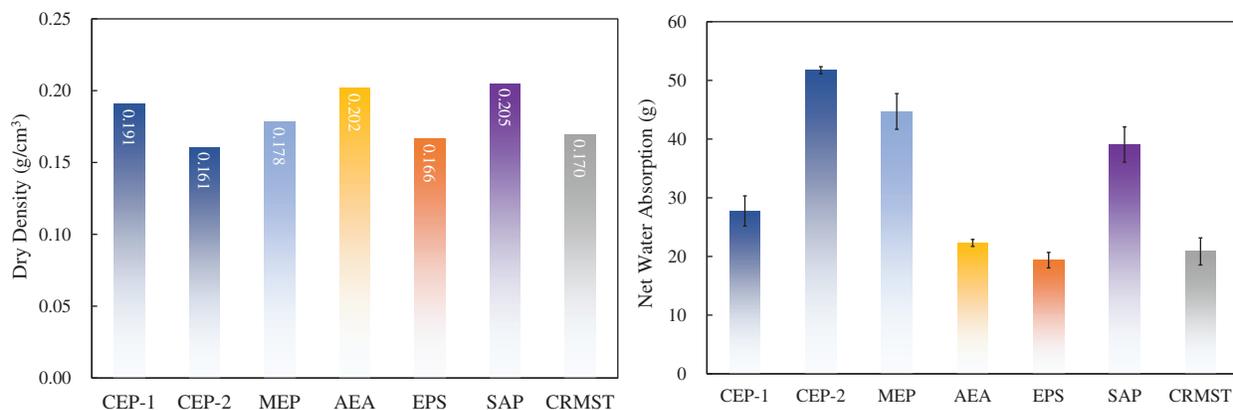
Figure 4: The dry density of the concrete/mortar prisms, and the net water absorption

The net water absorption is shown in the right subfigure of Fig. 4. It exhibits the expanded perlite (EP) aggregate concrete has the largest water absorption, which indicates the EP aggregate concretes have the highest porosity. Especially the coarse expanded perlite (CEP) aggregate concrete with the water dosage of 200 ml, which results from the microstructure of EP aggregate and voids inside the cement mortar paste. Then, the pore-induced mortars come the second, including AEA and SAP mortar. The water absorption of the expanded polystyrene (EPS) aggregate concrete and ceramsite aggregate concrete are comparably lower. The low water absorption of EPS aggregate concrete ascribes to the water hydrophobicity of EPS particle, while the CRMST aggregate concrete attributes the low water absorption to the dense texture of the ceramsite particle surface.

Combined with the dried density, it is inferred that the CEP concrete with 200 ml water has the lowest density and the most porous texture. On the contrary, the porous mortars have the highest density, but their porosity is comparatively higher than the EPS aggregate concrete and ceramsite aggregate concrete. EPS aggregate concrete and ceramsite aggregate concrete have a lower density but a lower porosity. The above experimental results are far from our expectation that a higher density means a lower porosity. Hence, the order of their thermal conductivity and mechanical strength would be complicated to analyze in the next context.

3.2 Mechanical Strength

3.2.1 The Flexural Strength

As we know, the mechanical performance of the cement-based composite is closely related to the water dosage. CEP-2 and MEP aggregate concrete were added with 200 ml water, which were more than the other specimens (160 ml). Their flexural strengths were the lowest among the 7 testing groups, as shown in Fig. 5. The MEP aggregate concrete exhibited a relatively higher flexural strength than CEP-2, which means a larger particle size aggregate decreased the concrete flexural strength.
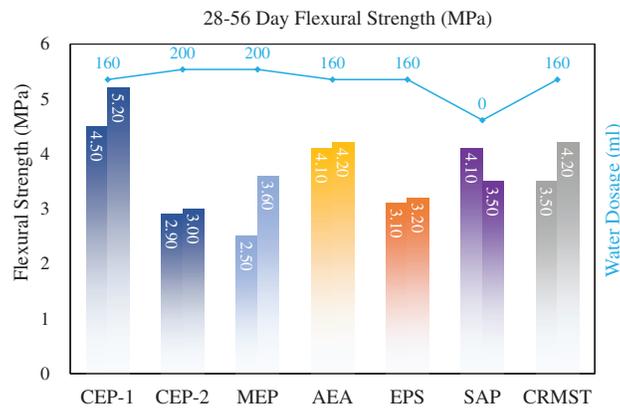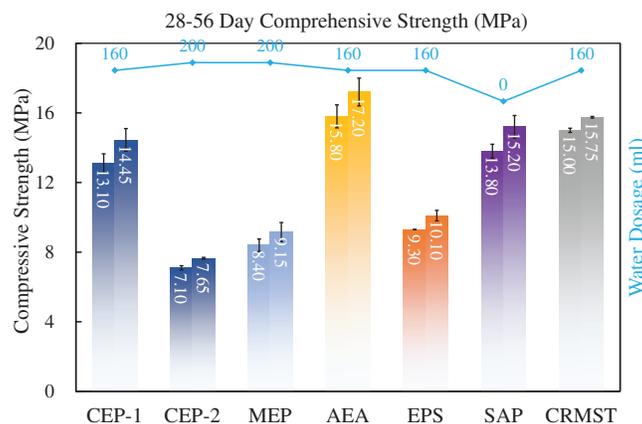

Figure 5: The flexural strength at 28 days and 56 days

Added with 160 ml water, the mechanical strength varied with the types of light aggregate in the concretes and the porous texture in the mortars. Combined with Table 2 and Fig. 5, it is found that CEP-1 aggregate concrete has the highest flexural strength, and the CRMST aggregate concrete comes the second. The EPS aggregate concrete has the lowest flexural strength. Hence, the organic aggregate concrete showed poorer flexural strength than inorganic aggregate concrete.

3.2.2 The Compressive Strength

The water dosage also affected the compressive strength. CEP-2 and MEP aggregate concrete added with 200 ml water have the lowest compressive strength, as shown in Fig. 6. Similarly, the MEP aggregate concrete exhibited a relatively higher compressive strength than CEP-2, which means a larger particle size of the EP aggregate also decreased the concrete compressive strength.


Figure 6: The compressive strength at 28 days and 56 days

Combined with Table 2 and Fig. 6, it is found that the compressive strength order among the cement composites in this study is different from that of the flexural strength. AEA mortar has the highest compressive strength, and the CRMST aggregate concrete comes the second. Then, the SAP mortar and CEP-1 aggregate concrete follow. The EPS aggregate concrete has the lowest compressive strength. Hence, the organic aggregate concrete also showed a poorer compressive strength than the inorganic aggregate concrete.

Among the light aggregate concrete, the mechanical strength of the ceramsite aggregate concrete is relatively higher. This is because the texture of the ceramsite particle is well structured. The crush strength of the ceramsite particle is higher than other aggregates. While the expanded perlite aggregate could be crushed into powder easily, and the EPS particle is elastic. Hence, the mechanical strength of the porous mortar is related to the porosity, and the mechanical strength of the light aggregate concrete is related to both the porosity and the innate strength of the aggregates.

3.3 Thermal Insulation

A lower value of thermal conductivity means a better thermal insulation, which is more suitably used as the construction material in cold region engineering. As shown in Fig. 7, EPS aggregate concrete has the poorest thermal insulation. The MEP aggregate concrete exhibits the best thermal insulation. This is because the water dosage for this group was 200 ml. The texture of the MEP aggregate concrete was the most porous.
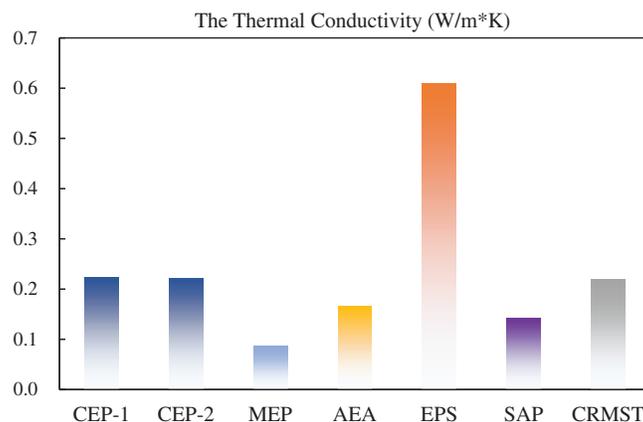
**Figure 7:** The thermal conductivity before the Freeze-Thaw cycle

The thermal insulation of the porous mortars come the second, then the ceramsite aggregate concrete and CEP aggregate concrete follow. Generally, the porous mortar shows a better thermal insulation than the light aggregate concretes. During the experimental process, it is found that the change of thermal conductivity after the Freeze-thaw cycle is not obvious, which is within the measuring errors of the thermal conductivity. Hence, the thermal insulation degradation during the Freeze-Thaw cycle was not discussed.

3.4 Mechanical Strength Loss under Freeze-Thaw Cycles

Flexural strength

Fig. 8 shows the flexural strength of the concrete/mortar prism. The left bar in the left subfigure denotes the flexural strength on the 56th day in the normal state, and the right bar denotes the flexural strength on the 56th day after the Freeze-Thaw cycle. In the right subfigure, the bar denotes the difference between the flexural strength in the normal state and after the Freeze-Thaw cycle. It is found that the flexural strength

of the CEP aggregate concrete was the most influenced by the Freeze-Thaw cycle, and EPS aggregate concrete was the least influenced. This is because the EPS is an elastic material, which could recover to its initial state after an environmental or mechanical disturbance.
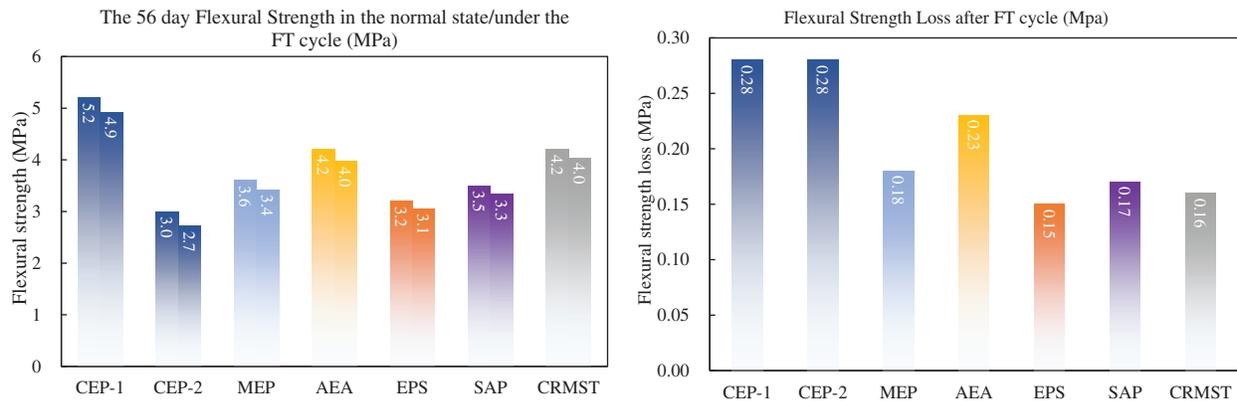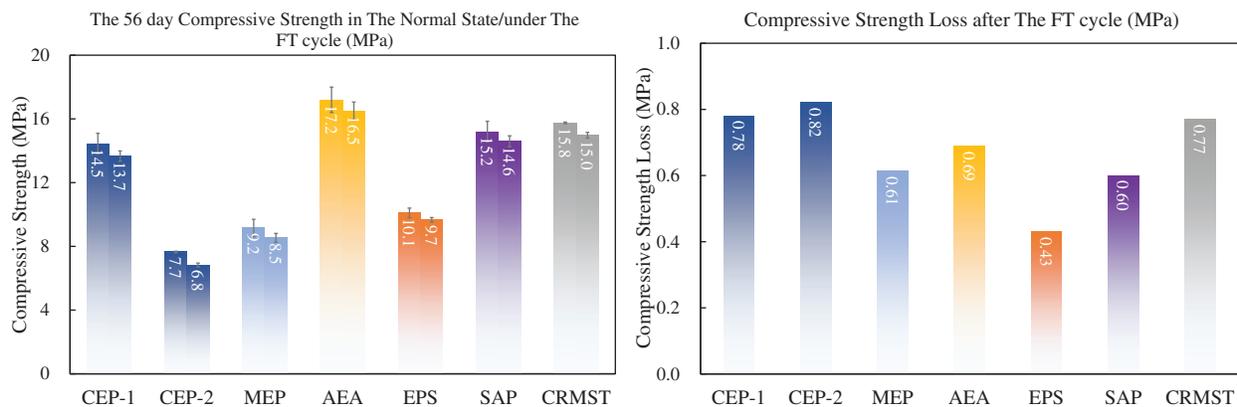

Figure 8: The flexural strength in the normal state and after the Freeze-Thaw cycle

Generally, the porous mortar showed a smaller flexural strength loss than the light aggregate concretes, except for the organic aggregate concrete (EPS). This ascribes to the developed microstructure of porous mortar paste, which has better frost resistance than the light aggregates. The perlite particles and ceramsite particles have a poor frost resistance, whose microstructure could be damaged under the Freeze-Thaw cycle. The comparison between the MEP and CEP aggregate concrete indicates that a smaller particle size of fragile inorganic aggregate has a better frost resistance.

Compressive strength

Fig. 9 shows the compressive strength of concrete/mortar prism in the normal state and under the Freeze-Thaw cycle. In the right subfigure, the bar denotes the difference between the compressive strength in the normal state and after the Freeze-Thaw cycle. Similar to the change of flexural strength, the CEP aggregate is still the most influenced. The ceramsite aggregate concrete comes the second.

Figure 9: The compressive strength in the normal state and after the Freeze-Thaw cycle

Generally, the frost resistance of the inorganic aggregate concrete is worse than the porous mortars. The EPS aggregate concrete is still the least influenced, which ascribes to the flexibility of EPS particles.

The compressive strength loss of the SAP mortar is also smaller than AEA mortar, which results from the internal curing of the expanded SAP hydrogel during the mortar hardening process. Hence, the microstructure is well developed. The compressive strength comparison between MEP and CEP aggregate concrete also verifies the inference that a smaller particle size of fragile inorganic aggregate has a better frost resistance.

The initial motivation to add the coarse aggregate is to improve the mechanical performance of the cement-based composite. While the addition of lightweight aggregate did not improve the mechanical strength. Moreover, the thermal insulation of the lightweight aggregate concretes is not as good as the porous mortars.

3.5 Combined Evaluation

3.5.1 The Standardized Comparison

In Fig. 10, it is found that more water addition would not deteriorate the entire performance of the expanded perlite aggregate concrete after the comparison between CEP-1 and CEP-2. A smaller size of perlite aggregate would improve the entire performance after the comparison between CEP-2 and MEP. The EPS aggregate concrete showed the best frost resistance. However, the poor mechanical strength and thermal insulation restrict its application in the cement-based composite. Compared with perlite, the ceramsite aggregate concrete has a balanced performance in mechanical strength, thermal insulation, and frost resistance.
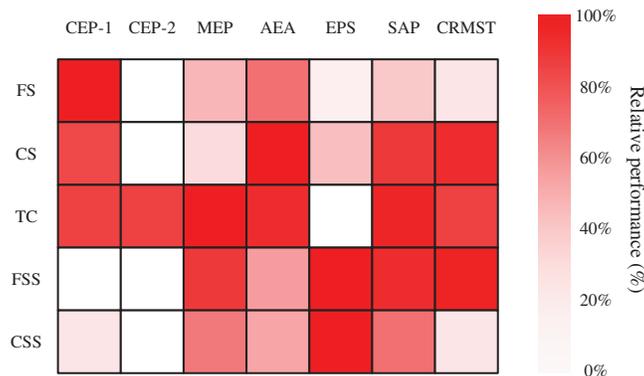

Figure 10: The standardized comparison of the cement-based composite in a cold environment

Generally, the porous mortars exhibited the best performance in the above five kinds of indices, which are better than the lightweight aggregate concrete. The mechanical strength of AEA mortar is relatively higher than the SAP mortar, while the frost resistance is not as good as SAP mortar. This phenomenon ascribes to the internal curing of expanded SAP hydrogel during the mortar hardening process, which developed the microstructure of mortar paste.

3.5.2 The Integral Comparison

As shown in Fig. 11, the holistic index indicates that the porous mortar is obviously better than the lightweight aggregate concretes. Among the lightweight aggregate concretes, the MEP aggregate concrete is the best, which is very close to SAP mortar. However, the KS loss after the Freeze-thaw cycle for the MEP aggregate concrete is the largest, which indicates its poorest frost resistance. The EPS aggregate concrete has the smallest value of KS. Hence, its working performance is the worst among these above cement composites, even it has the smallest KS loss.
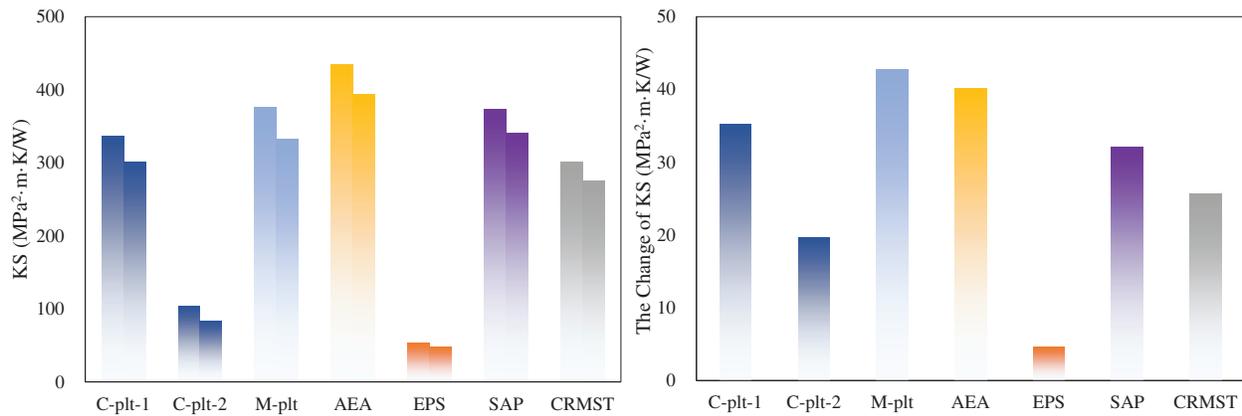
Figure 11: The holistic index of the cement-based composite used in this study

After comparison, the AEA mortar exhibits a better mechanical and thermal-insulating performance than SAP mortar. However, the KS loss after the Freeze-thaw cycle indicates the frost resistance of AEA mortar is not as good as SAP mortar, which has a developed microstructure. The conclusions here coincide with those inferred from Fig. 10, which confirms the reliability of the inferences that internal curing enhances the frost durability.

3.6 Microscopic Characterization

3.6.1 Optical Microscope

The optical microscope of the lightweight aggregate concretes and porous mortars were given in Fig. 12. The CEP-2 aggregate concrete added with more water exhibited more pores than the CEP-1 aggregate concrete. This explained why the mechanical strength of CEP-1 aggregate concrete was higher. The particle size of MEP aggregate is obviously smaller than CEP. The medium expanded perlite particle inside the MEP aggregate concrete paste is well-distribute, which results in a better thermal insulation than CEP aggregate concretes.
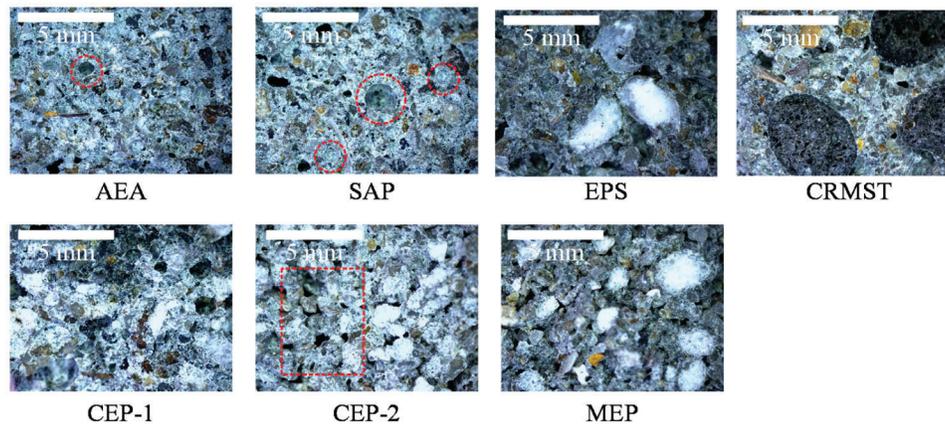
Figure 12: The optical microscope of the lightweight aggregate concretes and porous mortars

As for the porous mortars, their texture looks denser than the lightweight aggregate concretes by naked eyes in Fig. 2, which accords with the inference from the flexural/compressive strength in Figs. 5 and 6. The

optical microscope of the sectional profile disclosed that microstructure of the porous mortar is characterized with numerous voids. The lightweight aggregate concretes are characterized with dense mortar paste and loose aggregate. The loose aggregate mainly leads to the porosity of the lightweight aggregate concretes, which is generally higher than the porous mortars.

In the optical microscope, the void inside the porous mortars is spherical, while the void inside the lightweight aggregate concrete is an irregular shape. Obviously, the pore structure and paste connection for the porous mortar is better than the lightweight aggregate concrete, which leads to the higher mechanical strength than the lightweight aggregate concretes.

3.6.2 Scanning Electron Microscope

The SEM images of the CRMST aggregate concrete and EPS aggregate concrete are given in Figs. 13a and 13b are the microscope of CRMST aggregate concrete, and the ceramsite is colored in dark yellow. Figs. 13(c) and 13(d) are the microscope of EPS aggregate concrete, and the expanded polystyrene is colored in green.
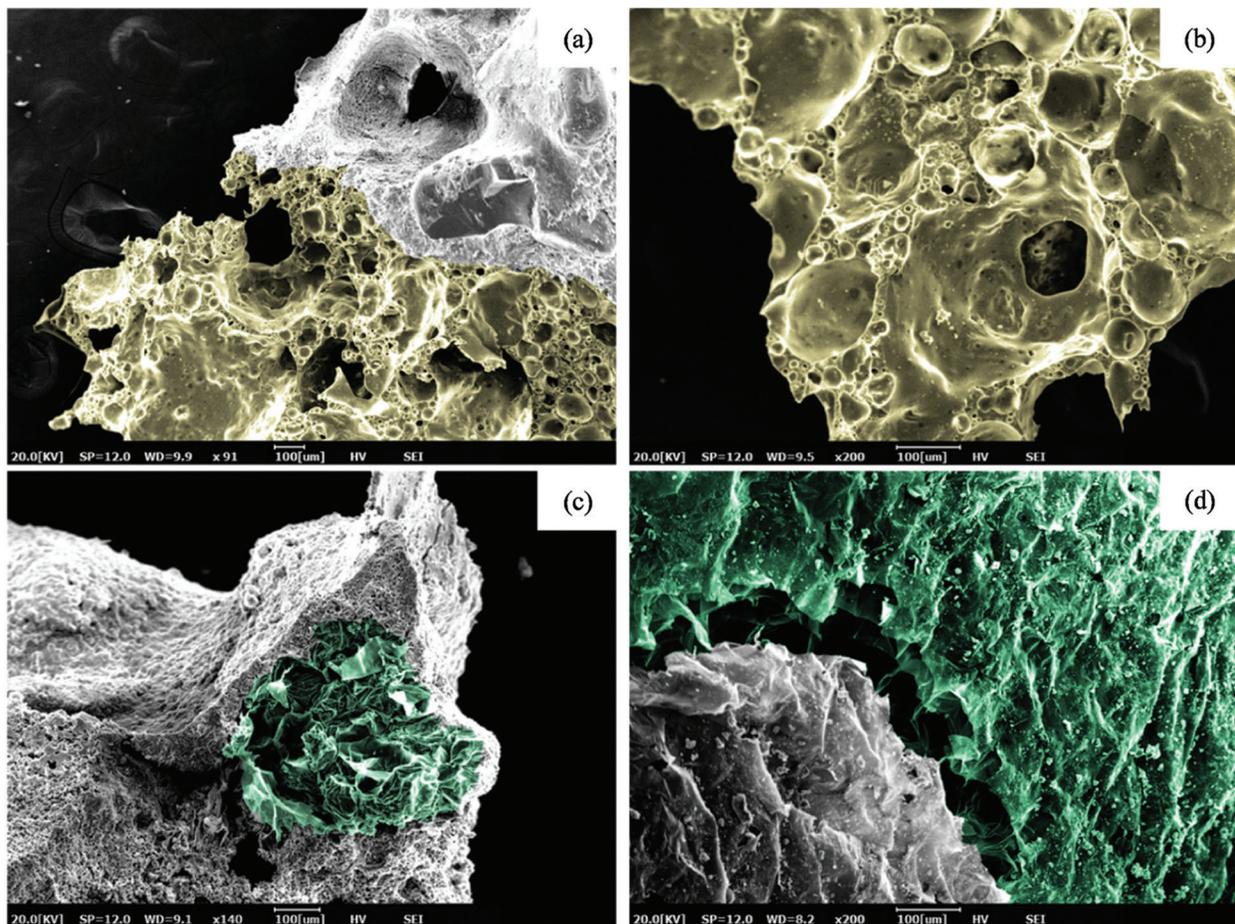

Figure 13: The SEM images of the CRMST aggregate concrete and EPS aggregate concrete

The microstructure of ceramsite inside the lightweight aggregate concrete is porous, and the voids of different diameters are scattered within the ceramsite particles. The section of ceramsite particle is a bit like cheese. While the microstructure of expanded polystyrene inside the lightweight aggregate concrete

is layered, which could recover under a mechanical disturbance. This microstructure explains why the EPS aggregate concrete exhibited better frost resistance.

The SEM images of the expanded perlite aggregate concrete, the SAP mortar, and the AEA mortar are given in Figs. 14a and 14b are the microscope of expanded perlite aggregate concrete, and the expanded perlite is colored in light brown. Fig. 14(c) is the microscope of the SAP mortar, and the expanded SAP induced cavity is colored in bright yellow. Fig. 14(d) is the microscope of AEA added mortar, the pore diameter is smaller and the pore shape is irregular.
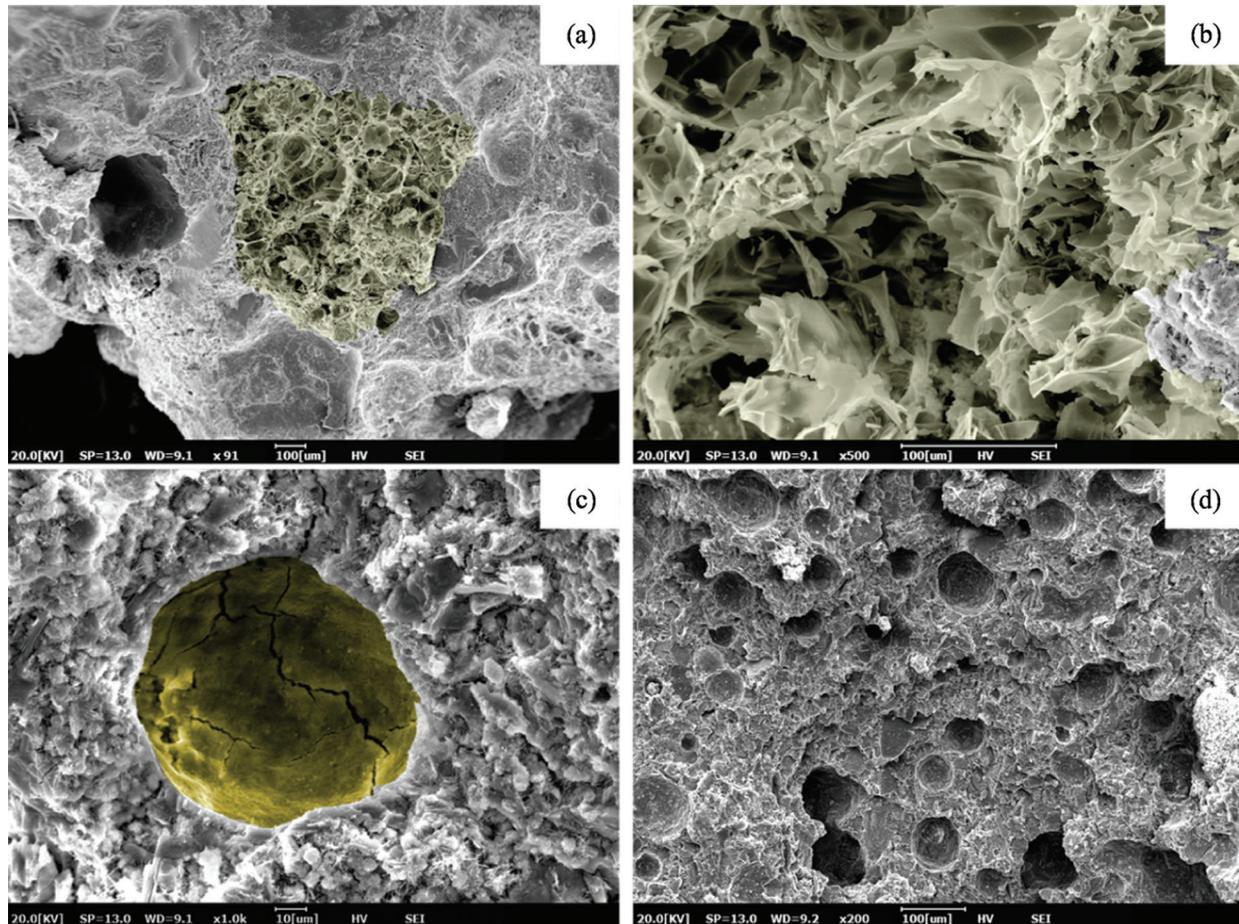
Figure 14: The SEM iamges of the expanded perlite aggregate concrete, SAP mortar, and AEA mortar

The microstructure of expanded perlite particles inside the lightweight aggregate concrete is like the scattered sheet. It shows poor mechanical strength, which could be crushed into powder by finger. The microstructure leads to an unsatisfactory frost resistance. In the Figs. 14c and 14d, the large-size cavity inside the SAP mortar and the scattered small-size voids inside the AEA mortar could be identified. It is found that the pores inside the LWAC are interconnected, while the pore inside the porous mortar is independent. The featured dissimilarity of microstructure between LWAC and porous mortar ascribe to their entire performance in cold environment.

It is also found the inner wall of SAP-induced cavity is well developed after the internal curing. Hence the mechanical strength of the cavity is higher than the void inside the AEA mortar. This explains why the frost resistance of the SAP mortar were better than the AEA mortar.

4 Conclusion

To investigate the thermal insulation and mechanical performance of lightweight aggregate concrete and porous mortar, the expanded perlite, ceramsite, and expanded polystyrene particles were added as aggregate, and the expanded SAP GEL and AEA agent were added to create the porous mortar. During the investigation process, the concrete/mortar was subjected to the Freeze-thaw cycle to test the mechanical strength loss, then the frost resistance could be obtained. Combined with the optical and Scanning Electronical Microscopic observation, several conclusions were obtained as follows:

a) As a fragile aggregate, the expanded perlite used in the cement-based material is recommended in small size, which could improve the concrete's entire performance in the cold environment.

b) A low water/binder ratio improves the entire performance of perlite aggregate concrete in the cold environment, including the mechanical strength, thermal insulation, and frost resistance.

c) The EPS aggregate concrete has the worst mechanical strength and thermal insulation, even it has a good frost resistance, which results from the flexibility of EPS particles.

d) Compared with lightweight aggregate concrete, the porous mortars have higher mechanical strength and better thermal insulation, and frost resistance.

e) The AEA mortar has a higher mechanical strength than SAP mortar, while the frost resistance is not as good as SAP mortar. The internal curing effect of expanded SAP hydrogel improves the durability under the Freeze-Thaw cycle.

Conflicts of Interest: The authors declare that they have no conflicts of interest to report regarding the present study.

Reference

1. Li, D., Wen, Z., Luo, J., Zhang, M., Chen, B. et al. (2019). Slope failure induced by cold snap and continuous precipitation in the seasonal frozen area of Qinghai-Tibet Plateau. *Science of the Total Environment, 694,* 133547. DOI 10.1016/j.scitotenv.2019.07.353.

2. Li, D., Zhang, M., Wen, Z., Chen, B., Xue, K. et al. (2021). Quantitative evaluation of characteristic precipitation event (CPE)'s effect on hydro-thermal state of active layer in Beiluhe area. *Natural Hazards, 105(3),* 1–20. DOI 10.1007/s11069-020-04401-1.

3. Li, D., Wen, Z., Cheng, Q., Xing, A., Zhang, M. et al. (2019). Thermal dynamics of the permafrost active layer under increased precipitation at the Qinghai-Tibet Plateau. *Journal of Mountain Science, 16(2),* 309–322. DOI 10.1007/s11629-018-5153-5.

4. Patton, A., Rathburn, S., Capps, D. (2019). Landslide response to climate change in permafrost regions. *Geomorphology, 340,* 116–128. DOI 10.1016/j.geomorph.2019.04.029.

5. Deng, D., Gao, S., Hu, L., Du, X., Wang, J. et al. (2016). The impact of Guizhou topography on the distribution of freezing rain in early January 2011. *Quarterly Journal of the Royal Meteorological Society, 141(693),* 3252–3267. DOI 10.1002/qj.2607.

6. Chen, T., Huang, W., Yoon, J. (2004). Interannual variation of the east asian cold surge activity. *Journal of Climate, 17(2),* 401–413. DOI 10.1175/1520-0442(2004)017<0401:IVOTEA>2.0.CO;2.

7. Hoerling, M., Kumar, A., Zhong, M. (1996). El Nino, La Nina, and the nonlinearity of their teleconnections. *Journal of Climate, 10(8),* 1769–1786. DOI 10.1175/1520-0442(1997)010<1769:ENOLNA>2.0.CO;2.

8. Li, Z., Huang, X., Yuan, D., Ma, Y. (2021). Study on characters of rural residential buildings based on the investigation in Shaanxi, Guangxi and Jiangsu in China. *E3S Web of Conferences*, vol. 237, pp. 3002. Zhangjiajie, China.

9. Takebayashi, H., Moriyama, M., Sugihara, T. (2012). Study on the cool roof effect of Japanese traditional tiled roof: Numerical analysis of solar reflectance of unevenness tiled surface and heat budget of typical tiled roof system. *Energy and Buildings, 55,* 77–84. DOI 10.1016/j.enbuild.2011.09.023.

10. Sinka, M., Sahmenko, G., Korjakins, A., Radina, L., Bajare, D. (2015). Hemp thermal insulation concrete with alternative binders, analysis of their thermal and mechanical properties. *Business Economy, 96,* 12029. DOI 10.1088/1757-899X/96/1/012029.

11. Chen, H. (2009). Influences of circular economy legislation on the building of resource-saving and environment-friendly society. *Journal of Wuhan University of Science and Technology (Social Science Edition), 11(5),* 72–77.

12. Lang, L., Liu, N., Chen, B. (2020). Strength development of solidified dredged sludge containing humic acid with cement, lime and nano-SiO$_2$. *Construction and Building Materials, 230,* 116971. DOI 10.1016/j. conbuildmat.2019.116971.

13. Ünal, O., Uygunoğlu, T., Yildiz, A. (2007). Investigation of properties of low-strength lightweight concrete for thermal insulation. *Building and Environment, 42(2),* 584–590. DOI 10.1016/j.buildenv.2005.09.024.

14. Pia, G., Sanna, U. (2013). A geometrical fractal model for the porosity and thermal conductivity of insulating concrete. *Construction and Building Materials, 44,* 551–556. DOI 10.1016/j.conbuildmat.2013.03.049.

15. Chen, B., He, M., Huang, Z., Wu, Z. (2019). Long-tern field test and numerical simulation of foamed polyurethane insulation on concrete dam in severely cold region. *Construction and Building Materials, 212,* 618–634. DOI 10.1016/j.conbuildmat.2019.04.016.

16. Liu, Y., Wang, W., Zhang, Y., Li, Z. (2015). Mechanical properties of thermal insulation concrete with a high volume of glazed hollow beads. *Magazine of Concrete Research, 67(13),* 693–706. DOI 10.1680/macr.14.00296.

17. Gu, K., Chen, B. (2020). Loess stabilization using cement, waste phosphogypsum, fly ash and quicklime for self-compacting rammed earth construction. *Construction and Building Materials, 231,* 117195. DOI 10.1016/j. conbuildmat.2019.117195.

18. Demirboğa, R. (2007). Thermal conductivity and compressive strength of concrete incorporation with mineral admixtures. *Building and Environment, 42(7),* 2467–2471. DOI 10.1016/j.buildenv.2006.06.010.

19. Sargam, Y., Wang, K., Alleman, J. (2020). Effects of modern concrete materials on thermal conductivity. *Journal of Materials in Civil Engineering, 32(4),* 04020058. DOI 10.1061/(ASCE)MT.1943-5533.0003026.

20. Marie, I. (2017). Thermal conductivity of hybrid recycled aggregate–Rubberized concrete. *Construction and Building Materials, 133,* 516–524. DOI 10.1016/j.conbuildmat.2016.12.113.

21. Zhai, X., Yan, J., Cao, C. (2021). Seismic performance and flexible connection optimization of prefabricated integrated short-leg shear wall filled with ceramsite concrete. *Construction and Building Materials, 311,* 125224. DOI 10.1016/j.conbuildmat.2021.125224.

22. Taher, S., Saadullah, S., Haido, J., Tayeh, B. (2021). Behavior of geopolymer concrete deep beams containing waste aggregate of glass and limestone as a partial replacement of natural sand. *Case Studies in Construction Materials, 15,* e00744. DOI 10.1016/j.cscm.2021.e00744.

23. Wang, X., Wu, D., Geng, Q., Hou, D., Wang, M. et al. (2021). Characterization of sustainable ultra-high performance concrete (UHPC) including expanded perlite. *Construction and Building Materials, 303,* 124245. DOI 10.1016/j.conbuildmat.2021.124245.

24. Souza, T., Lima, V., Araújo, F., Miranda, L., Melo Neto, A. (2021). Alkali-activated slag cellular concrete with expanded polystyrene (EPS)–physical, mechanical, and mineralogical properties. *Journal of Building Engineering, 44,* 103387. DOI 10.1016/j.jobe.2021.103387.

25. Kim, K., Shin, M., Cha, S. (2013). Combined effects of recycled aggregate and fly ash towards concrete sustainability. *Construction and Building Materials, 48,* 499–507. DOI 10.1016/j.conbuildmat.2013.07.014.

26. Yasar, E., Atis, C., Kilic, A., Gulsen, H. (2003). Strength properties of lightweight concrete made with basaltic pumice and fly ash. *Materials Letters, 57(15),* 2267–2270. DOI 10.1016/S0167-577X(03)00146-0.

27. Li, D., Chen, B., Chen, X., Fu, B., Wei, H. et al. (2020). Synergetic effect of superabsorbent polymer (SAP) and crystalline admixture (CA) on mortar macro-crack healing. *Construction and Building Materials, 247,* 118521. DOI 10.1016/j.conbuildmat.2020.118521.

28. Campbell-Allen, D., Thorne, C., Zoldners, N., Malhotra, V. (1963). The thermal conductivity of concrete. *Magazine of Concrete Research, 15(43),* 39–48. DOI 10.1680/macr.1963.15.43.39.

29. Gu, K., Chen, B. (2020). Research on the incorporation of untreated flue gas desulfurization gypsum into magnesium oxysulfate cement. *Journal of Cleaner Production, 271,* 122497. DOI 10.1016/j.jclepro.2020.122497.

30. Siengsanoh, K., Limkitjaroenporn, P., Kaewkhao, J. (2021). Porosity investigation of bricks by gamma-ray transmission measurement. *Materials Today: Proceedings, 43,* 2612–2617. DOI 10.1016/j.matpr.2020.04.624.

31. Li, D., Chen, B., Xue, K., Li, A., Zheng, H. et al. (2021). Durability and mechanical performance of pure/chelated superabsorbent polymer (SAP/SAPC) added mortar in cold region. *Journal of Building Engineering, 44,* 102982. DOI 10.1016/j.jobe.2021.102982.